1863

RFP-1706
June 30, 1971

MASTER

NEUTRON RADIOGRAPHY WITH A SEALED-TUBE NEUTRON GENERATOR AND GRAPHITE MODERATED SYSTEM

Dennis Vasilik
Richard Murri

Dow
®

DISCLAIMER

This report was prepared as an account of work sponsored by an agency of the United States Government. Neither the United States Government nor any agency Thereof, nor any of their employees, makes any warranty, express or implied, or assumes any legal liability or responsibility for the accuracy, completeness, or usefulness of any information, apparatus, product, or process disclosed, or represents that its use would not infringe privately owned rights. Reference herein to any specific commercial product, process, or service by trade name, trademark, manufacturer, or otherwise does not necessarily constitute or imply its endorsement, recommendation, or favoring by the United States Government or any agency thereof. The views and opinions of authors expressed herein do not necessarily state or reflect those of the United States Government or any agency thereof.

DISCLAIMER

Portions of this document may be illegible in electronic image products. Images are produced from the best available original document.

NEUTRON RADIOGRAPHY WITH A SEALED-TUBE
NEUTRON GENERATOR AND GRAPHITE
MODERATED SYSTEM

Dennis Vasilik

Richard Murri

CONTENTS

LIST OF FIGURES

NEUTRON RADIOGRAPHY WITH A SEALED-TUBE NEUTRON GENERATOR AND GRAPHITE MODERATED SYSTEM

Dennis Vasilik and Richard Murri

Abstract. Neutron radiographs of good quality have been produced by using a sealed-tube neutron generator and a graphite moderator system. The graphite moderator is a right-cylinder 76.2 cm in diameter and 76.2-cm high. A thermal neutron flux at the object of 1.1×10^5 n/cm^2-sec and a cadmium ratio of 3.5 was measured. The collimator ratio was 7.25; the X-ray intensity was 0.50 mr/sec; and the resolution was measured to be 0.025 cm. Experimental techniques for determining fast and thermal neutron fluences are also described.

INTRODUCTION

A thermal neutron radiography system using an accelerator neutron source with a graphite moderator was developed and studied. A nuclear reactor is the most intense source of thermal neutrons and is therefore ideal for neutron radiography. However, an accelerator has two advantages over a reactor neutron source: it is relatively inexpensive, and it is portable. Also, the use of an accelerator enables neutron radiography to be used in laboratories which do not have a reactor.

Radiography is defined as the use of radiant energy for the nondestructive examination of opaque objects. A collimated beam of intense energy is passed through an object. This beam is differentially attenuated by the elements which make up the internal structure of the object. An image of the internal structure of the object is then imprinted in the beam. This information is recorded on commercial X-ray film and used to indicate the comparative reliability of the object being tested.

Neutron radiography can be used by the industrial radiographer to image objects that X-rays can image only with difficulty, if at all. This capability exists because absorption of neutrons in matter is different from absorption of X-rays.

In general, the laws governing the attenuation of neutrons in matter are similar in form to those laws governing the attenuation of X-rays in matter. The fundamental exponential attenuation law $I_n = I_o e^{-\mu x}$, is applicable to either neutrons or X-rays in matter. I_o is the intensity of

an incident beam of either form of radiation, and I_x is the intensity of the transmitted portion of the beam at a given thickness, x, of matter. The absorption coefficient, μ, is a function of the energy of the incident radiation. The utility of neutron radiography is characterized by the large differences in values of μ for neutrons. Thermal neutrons are used in most radiography work because neutrons in this energy range (0.01 – 0.3 eV) are relatively easy to detect photographically and have desirable attenuation characteristics.

In Figure 1, the mass absorption coefficient for thermal neutrons and X-rays is plotted against the atomic number of most of the elements. The mass absorption coefficient (μ/ρ) is the absorption coefficient divided by the density of the element.

The solid line in Figure 1 represents the behavior of the mass absorption coefficient for a given X-ray energy. It is seen that the ability of the elements to attenuate X-rays increases approximately exponentially with the atomic number.

The mass absorption coefficients for thermal neutrons, however, are random when plotted against atomic number. These differences in mass absorption coefficients account for the versatility of thermal neutron radiography.

Light elements such as boron, hydrogen, lithium, and beryllium strongly attenuate thermal neutrons but are essentially transparent to X-rays. Also, elements such as lead and aluminum are transparent to thermal neutrons but attenuate X-rays strongly.

Therefore, using thermal neutron radiography, the height of a column of water in a lead tube can be determined. The lead is transparent to the neutrons whereas the water strongly attenuates them. X-rays, however, are attenuated strongly in lead, and the additional slight attenuation caused by water would be difficult to detect.

Figure 1 shows another interesting feature of thermal neutron radiography. Elements that are close to each other on the periodic chart are difficult to distinguish by means of X-rays. However, these same elements usually have very different
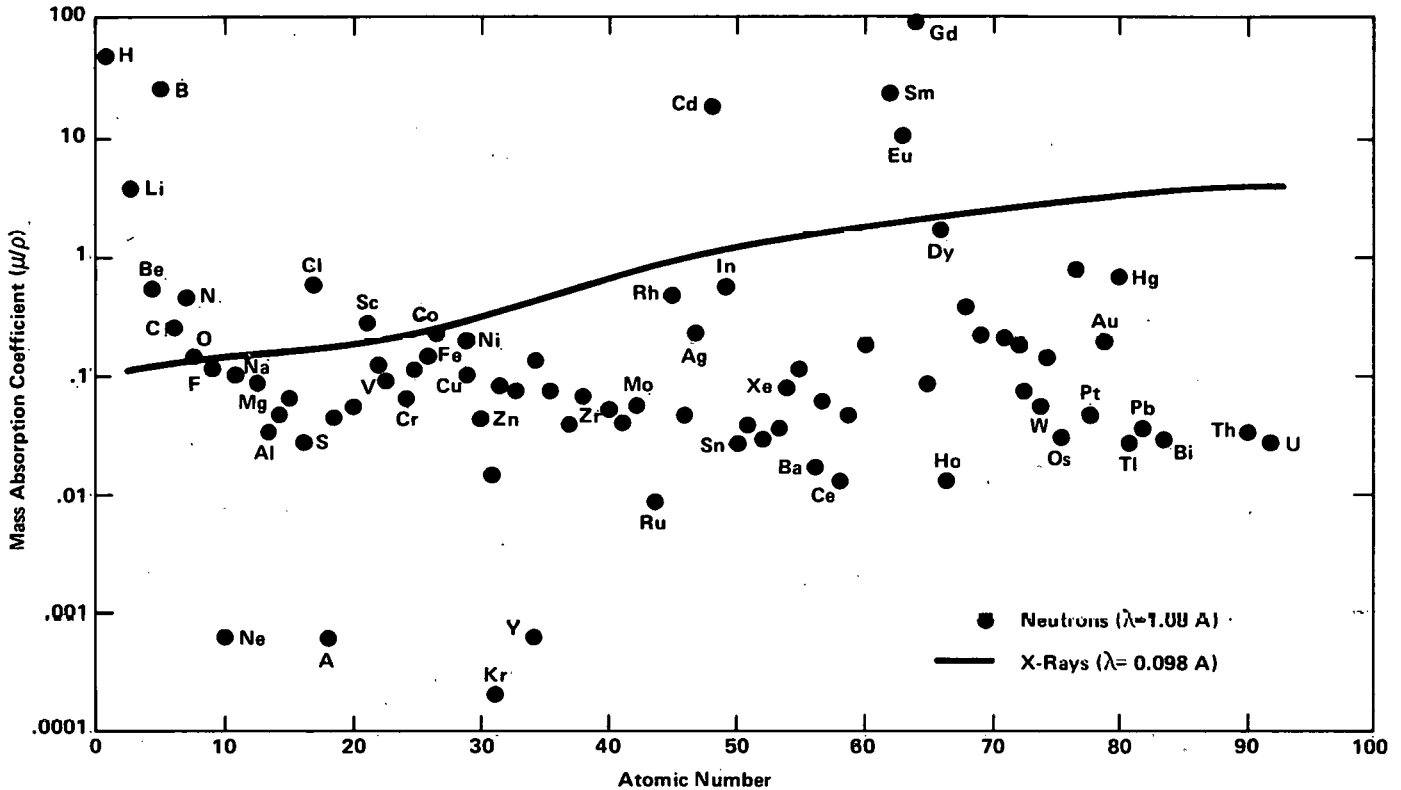
Figure 1. Mass Absorption Coefficients (cm²/g) of the Elements for X-rays and Thermal Neutrons.

characteristics for thermal neutrons. Cadmium, which has an atomic number of 48, is difficult to distinguish from tin of atomic number 50 by means of X-rays. However, the mass absorption coefficient of cadmium is 1,000 times larger than the mass absorption coefficient of tin. These two elements are easily distinguished by thermal neutron radiography.

As another example, consider the inspection of fuel elements of a nuclear reactor for the presence of uranium isotopes. Using X-rays, it would be impossible to distinguish between ^{235}U and ^{238}U. However, using thermal neutrons, this would be an easy task; ^{235}U has a thermal neutron cross section of 678 barns, whereas ^{238}U has a cross section of only 2.73 barns.

SUMMARY

Investigations of a thermal radiography system which uses graphite as the moderating material and an accelerator as the neutron source show the $He^3(d,n)He^4$ and $H^2(H^3,n)He^4$

reactions to be suitable for some commercial nondestructive testing applications. One of the biggest problems in the development and use of neutron radiography has been the lack of inexpensive systems which are portable, reliable, and easy to operate. Although graphite is a material of relatively low moderating ability, the system has a thermal neutron beam of sufficient intensity and collimation to produce useful radiographs of test objects limited to approximately 5 cm in thickness. Neutron fluences of 1.1×10^5 n/cm²-sec have been obtained at the test-object position. Resolution, using a collimator ratio of 7.25, was 0.025 cm for a film-to-IQI separation of 0.064 cm. Experience has shown that the advanges advantages of the sealed-tube generator and graphite moderator system are:

1. Simple construction and operation

2. Good radiographic resolution

3. Low cost (relative to a reactor)

4. Excellent thermal neutron/gamma ratio

5. Acceptable exposure times

6. Safety of operations and ease of maintenance

The capabilities of the system reported in this paper could be utilized successfully by many industries for low-volume, on-line inspection. Large volume inspection requirements could be achieved by modifying the system to include multiple beam-extraction voids. Examples of applications which could make use of the graphite system are:

1. Inspection of ordnance devices

2. Determination of hydrogen content in various materials

3. Inspection of materials which are close in density or atomic number

4. Evaluation of metal assemblies which contain organic components

5. Studies of biological specimens

6. Inspection of reactor fuel elements and control rods

7. Inspection of certain low density components imbedded in a high density matrix

The graphite moderator system with its limited beam intensity cannot provide the resolution or detail capability of the modern day reactor but acceptable results can be achieved for many applications.

It has been shown that a graphite moderator can be used with an accelerator neutron source to provide a thermal neutron radiography system capable of being used for a variety of industrial applications. In addition, an attempt has been made to enumerate a number of experimental measurements and system parameters required in a report when studying nonreactor neutron radiography systems. These include:

1. Thermal neutron flux distribution inside of the bare moderator system along a given axis of symmetry

2. Fast neutron source yield

3. Cadmium ratio of both the beam and of the moderator

4. Ratio of the thermal neutron beam flux to the intensity of X-rays in the beam

5. Radiographic resolution measured with a standard IQI[11]

6. Collimator ratio for each radiograph reported

7. Exposure time for each radiograph reported

8. Response of each film investigated to the neutron beam (film density as a function of exposure time)

9. Physical dimensions of the neutron radiography system (to include moderator, collimator, and shielding)

Nonreactor neutron radiography investigations to date have been relatively few in number, [1-4,8,9,11-14] but private communications by the authors have shown that research and development in the science and application of nonreactor radiography is being vigorously pursued. As more nonreactor systems are evaluated and reported, it is imperative that certain criteria be established for the purpose of allowing each investigator to adequately compare his results against the results of others. Nonreactor neutron radiography must be standardized so that it can be properly applied in the industrial nondestructive testing facility. Those items enumerated above should provide a minimum foundation for all future reports in this area.

The results of these investigations have provided the basis for futher studies in thermal neutron radiography with an accelerator neutron source. Additional work is required to improve beam extraction and system shielding. Preliminary studies show that significant improvements in beam intensity result from the use of water or beryllium as the moderating material. In addition, depleted and enriched uranium geometries around the source are being studied to determine an optimum multiplication factor from fission (n,2n) and (n,3n) reactions caused by thermal and fast neutrons.

REVIEW OF THE LITERATURE

Since the discovery of the neutron by Chadwick in 1932, it has been known that neutrons can be used to make radiographic images. In 1935, Kallmann[1] was credited with taking the first neutron radiographs by using a water moderator and a low-yield accelerator source, which yielded nearly 4×10^7 n/sec. Exposure times were 4 to 5 hours and the radiographs had poor quality.

During the 1950's, work was performed in England by Thewlis, [2,3] and in Germany by Peter,[4] using a higher yield accelerator source than used by Kallman. Radiographs of reasonable quality were obtained with exposure times of 1 to 3 minutes. Thewlis and Derbyshire[5] are credited with conducting the first investigations into neutron radiography using a reactor as the neutron source.

Since 1960, the demands of nondestructive testing have provided the impetus for the development and wide use of neutron radiography in industry.[6,7] Berger [8] published the definitive work on the methods, capabilities, and applications of neutron radiography.

In nonreactor studies, Shaw and Cason [9] used ^{252}Cf for the neutron radiography of rifle ammunition. Investigations have been conducted within the past few years with water or paraffin moderators by Iddings,[10] Barton[11] Berger,[6] Wood,[12] and Breynat and Dubus.[13] Some interesting aspects of beam design for nonreactor radiography systems are discussed by Barton.[14]

NEUTRON SOURCE

A Kaman Nuclear A-711 neutron generator is used as a source of neutrons having an energy of approximately 14.3 MeV. In this tube, a continuous yield of neutrons is generated from $H^3(d,n)He^4$ and $H^2(H^3,n)He^4$ reactions. These reactions are produced by deuterium and tritium gases which are ionized by a Penning-ion-gage type source and accelerated into a grounded target assembly by a potential of 190 to 200 kV. The target consists of a layer of titanium in which tritium (7 curies) and deuterium are absorbed. The neutron yield of the generator was determined to be 7.72×10^{10} n/sec by a copper activation analysis technique.

The generator, shown in Figure 2, is a cylinder 25.4 cm in diameter and 58.96-cm long. When used with a graphite moderator, thermal neutrons necessary for neutron radiography are provided.
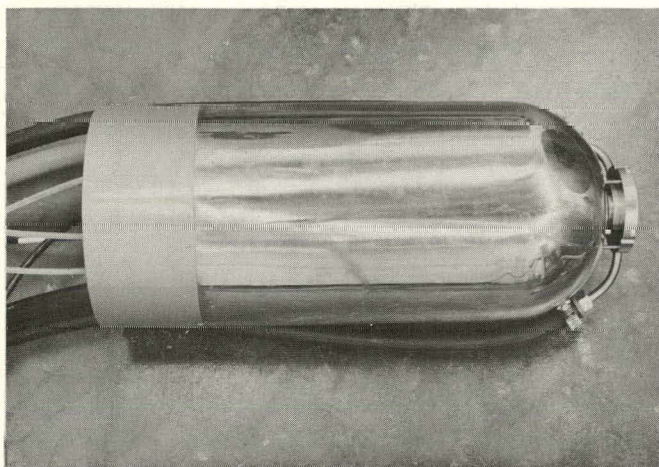
Figure 2. Sealed-Tube Neutron Generator.

MEASUREMENT OF NEUTRON FLUENCES

As part of the investigations to develop neutron radiography using a neutron generator, it was necessary to measure the fast neutron yield of the generator and the thermal neutron fluences produced by the graphite moderator which surrounds the fast neutron source. A method of foil activation analysis was chosen for these measurements. The formulae derived relate neutron flux to the number of counts registered by a counting system. The formulae also take into account irradiation time, transfer time, counting time, area and thickness of foil, type of foil, and various counting factors. These factors are discussed and the method of determining each factor is explained.

Theory

It is possible to measure the intensity of a neutron flux by taking advantage of certain neutron absorption reactions which lead to the formation of radioisotopes whose activity can be determined by gamma counting. The activity of an irradiated sample is directly related to the neutron flux.

Derivation of Flux Relationships. A thin foil of known physical and nuclear properties is irradiated by neutrons for a given time t_o. The foil is then removed from the flux and transferred to a counter where the activity of the foil is measured. Figure 3 shows the time sequence for this procedure.

Figure 3. Activation Analysis Sequence.
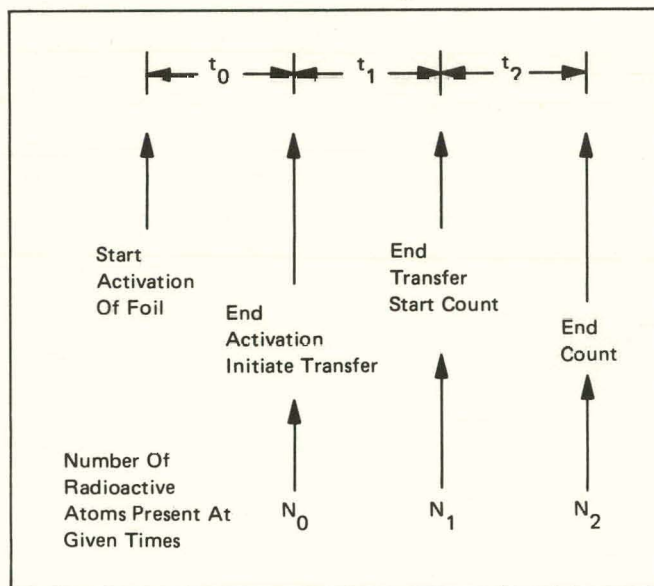
The rate at which neutrons in the beam interact with nuclei in the foil in a small thickness, dx, at the position x (measured from the front face of the foil) is approximated by

$$dR = \phi(x) n_t \sigma_t dx, \qquad (1)$$

where n_t is the total number of nuclei per cm^3, σ_t is the total microscopic neutron cross section in cm^2, $\phi(x)$ is the neutron flux in n/cm^2-sec, and R is number/cm^2-sec. A microscopic cross section σ, is a measure of the probability of the occurrence of a particular nuclear reaction under given conditions. For the particular case stated, σ_t represents the probability that all possible nuclear reactions will occur under the given experimental conditions.

The flux is not constant throughout the foil but is equal to the incident flux minus the rate at which neutrons have been removed from the beam by interactions with nuclei in a thickness x of the foil. That is:

$$\phi(x) = \phi_o - R(x) \qquad (2)$$

Substituting Equation 2 into Equation 1 gives

$$dR = (\phi_o - R) n_t \sigma_t dx,$$

or

$$\frac{dR}{\phi_o - R} = n_t \sigma_t dx.$$

Integrating over the thickness of the foil,

$$\ln(\phi_o - R) = -n_t \sigma_t x + C.$$

At $x = 0$, $R = 0$, so $C = \ln\phi_o$ and the above equation becomes

$$\ln(\phi_o - R) - \ln\phi_o = -n_t \sigma_t x.$$

This can be rewritten as

$$R = \phi_o(1 - e^{-n_t \sigma_t x}).$$

The total rate at which neutrons interact with the nuclei in the foil is therefore

$$RA = \phi_o A(1 - e^{-n_t \sigma_t x}), \qquad (3)$$

where A is the area of the foil. Equation 3 gives the total interaction rate which includes scattering events and many types of absorption reactions. The actual activity that is measured in the foil is produced by one particular nuclear reaction. Therefore, it is the rate at which this particular reaction is occurring, not the total rate as given in Equation 3, that must be related to the activity in the foil.

The particular reaction rate is obtained by multiplying the total rate (Equation 3) by the relative probability that the desired reaction will occur. This relative probability is the ratio of the macroscopic cross section Σ_p for the particular reaction to the total macroscopic cross section Σ_t. A macroscopic cross section Σ is equal to the product of the microscopic cross section σ and the total number of nuclei per unit volume, n. The rate at which particular nuclei are being activated in a specific way is given by

$$R_p A = \phi_o A(1 - e^{-n_t \sigma_t x}) \frac{\Sigma_p}{\Sigma_t},$$

where the subscript p refers to the particular reaction of interest.

The above equation can be written as

$$R_p A = \phi_o A(1 - e^{-n_t \sigma_t x}) \frac{n_p \sigma_p}{n_t \sigma_t}. \qquad (4)$$

During activation, the rate of change of the number N of activated nuclei is equal to the rate at which they are formed minus the rate at which they decay. Thus,

$$\frac{dN}{dt} = RA - \lambda N,$$

where λ is the decay constant.

This can be arranged to the form

$$\frac{dN}{\left(\frac{RA}{\lambda} - N\right)} = \lambda dt.$$

Integrating,

$$\ln\left(\frac{RA}{\lambda} - N\right) = -\lambda t + C.$$

At $t = 0$, $N = 0$, so $C = \ln(RA/\lambda)$ and then this equation can be written as

$$\ln\left(\frac{\frac{RA}{\lambda} - N}{\frac{RA}{\lambda}}\right) = -\lambda t,$$

or

$$N = \frac{RA}{\lambda}(1-e^{-\lambda t}) \ .$$

If we let $N = N_o$ at the end of irradiation ($t = t_o$), then the above equation becomes

$$N_o = \frac{RA}{\lambda}(1 - e^{-\lambda t_o}). \qquad (5)$$

During transfer from the neutron irradiation position to the gamma counter, the rate of decay is

$$\frac{dN}{dt} = -\lambda N,$$

where $t = 0$ is now defined to be at the start of transfer.

Integrating, this becomes

$$\ln N = -\lambda t + C.$$

At $t = 0$, $N = N_o$, so $C = \ln N_o$ and

$$\ln \frac{N}{N_o} = -\lambda t,$$

or

$$N = N_o e^{-\lambda t}.$$

At $t = t_1$, $N = N_1$; thus,

$$N_1 = N_o e^{-\lambda t_1}. \qquad (6)$$

Similarly, during counting, the rate of decay is $(dN/dt) = -\lambda N$ where $t = 0$ is now defined to be at the start of counting. Using the conditions that at $t = 0$, $N = N_1$ and at $t = t_2$, $N = N_2$ the result is

$$N_2 = N_1 e^{-\lambda t_2}. \qquad (7)$$

The number of atoms which decay during time t_2 is just $N_1 - N_2$. Denoting this by N_T,

$$N_T = N_1 - N_2 = N_1(1 - e^{-\lambda t_2}).$$

Substituting for N_1 and N_o using equations 5, 6, and 7 results in

$$N_T = \frac{R_p A}{\lambda}(1 - e^{-\lambda t_o})e^{-\lambda t_1}(1 - e^{-\lambda t_2}).$$

Using (4) this becomes

$$N_T = \frac{\phi_o A n_p \sigma_p(1-e^{-n_t\sigma_t X})}{n_t\sigma_t\lambda}(1-e^{-\lambda t_o})e^{-\lambda t_1}(1-e^{-\lambda t_2}). \qquad (8)$$

Equation 8 is an expression for the true number of atoms which decay during the counting period t_2.

N_T is also related to the number of counts, C, obtained by counting the activated foil.[15] When gamma counting is used in the analysis, the area of a particular photopeak is determined from the gamma spectrum. This area C is related to N_T by correcting for photopeak efficiency P, branching ratio ϵ, absorption correction factor a, and detector efficiency q. These factors are explained in the next section. The relation between N_T and C is:

$$N_T = C/P\epsilon aq.^{[15]}$$

Substituting in Equation 8 one obtains

$$\frac{C}{P\epsilon aq} = \frac{\phi_o A n_p \sigma_p}{n_t\sigma_t\lambda}(1-e^{-\sigma_t n_t X})(1 - e^{-\lambda t_o})e^{-\lambda t_1}(1 - e^{-\lambda t_2}),$$

or

$$\phi_o = \frac{n_t\sigma_t\lambda C}{P\epsilon aq A n_p \sigma_p(1-e^{-\sigma_t n_t X})(1 - e^{-\lambda t_o})e^{-\lambda t_1}(1 - e^{-\lambda t_2})}. \qquad (9)$$

This expression gives the neutron flux in neutrons per cm^2-sec as a function of the number of counts (C) in a certain photopeak measured during counting time t_2.

Explanation of Counting Factors. As given previously, the relationship between N_T and C is $N_T = C/P\epsilon aq$.

● P- is the photopeak efficiency or sometimes called the peak-to-total ratio. A gamma ray interacts with a NaI (Tl) detector in three primary ways: (1) photoelectric effect, (2) Compton effect, or (3) pair production. P is the ratio of the number of gammas of a certain energy interacting by the photoelectric effect to the number of gammas of the same energy interacting by all other processes. P is dependent on the energy of the gamma ray and the size of the detector. The factor can be measured experimentally or obtained from published data.[16]

● ϵ- is the branching ratio. This is the number of gamma rays of a certain energy emitted per decay of the activated nuclide. This factor is obtained by studying the decay scheme of the nuclide of interest.

● a- is the gamma-ray absorption correction factor. It is composed of two parts. One part corrects for self absorption in the foil and the other corrects for absorption in an absorber. Both are calculated in the same way. If an absorber is present between the foil and the detector, it will interact with some of the gamma rays coming from the foil, preventing them from reaching the detector. The a is computed by determining the ratio of the intensity of gammas of a given energy passing through the absorber to the intensity of the gammas of the given energy incident on the absorber. This is expressed as[17]

$$a = \frac{I}{I_o} = B_f B_a e^{(-\mu_f \rho_f \Delta \xi_f - \mu_a \rho_a \Delta \xi_a)}$$

where B is the dose buildup factor,[17] μ is the mass attenuation coefficient, ρ is the density of the absorber, and $\Delta \xi$ is the absorber thickness. The subscripts f and a represent the foil and absorber respectively. Since we are concerned only with a certain energy gamma ray passing through the absorber, the dose buildup factors $B_f = B_a = 1.0$.[17]

● q- is the detector efficiency. It is a measure of the ability of the detector to detect the radiation coming from the radioactive source. It is a combination of a geometric factor and the probability that a certain energy photon will be absorbed in the detector. For a thin disk source of radius R placed at a height h_o above a NaI (Tl) crystal of radius r_o, and thickness t_o, the detector efficiency is given by[16]

$$q = \frac{1}{\pi R^2} \int_0^R x dx \int_{-\pi/2}^{\pi/2} d\phi \left\{ \int_0^{\theta_1} (1-e^{-\tau \cdot t_o/\cos \theta}) \sin \theta d\theta \right.$$

$$\left. + \int_{\theta_1}^{\theta_2} \left(1-e^{-\tau \cdot (x/\sin \theta - h_o/\cos \theta)}\right) \sin \theta d\theta \right\} .$$

The derivation of the above equation and an explanation of the symbols is given in Appendix I. For a disk of finite thickness, the detector efficiency is

$$q = \frac{1}{\pi R^2 t} \int_0^t dy \int_0^R x dx \int_{-\pi/2}^{\pi/2} d\phi \left\{ \int_0^{\theta_1} (1-e^{-\tau \cdot t_o/\cos \theta}) \sin \theta d\theta \right.$$

$$\left. + \int_{\theta_1}^{\theta_2} \left(1-e^{-\tau \cdot (x/\sin \theta - h_o/\cos \theta)}\right) \sin \theta d\theta \right\} .$$

In Appendix II, a FORTRAN IV computer program was written for the numerical integration of the above equation to calculate q. Therefore, one can calculate the detector efficiency for any experimental arrangement of crystal and detector foil.

Examples of Method

It is desirable for this study to measure both the fast neutron output of the generator and thermal neutron fluences. These two measurements will be discussed separately.

The counting apparatus used for these measurements is shown in Figure 4. A complete gamma spectrum of a radioactive foil is first acquired on a multichannel analyzer. The photopeak of interest is then integrated directly by the analyzer and this number is read out. When the background is subtracted, one is left with C as given by equation 9. Analyzer dead-time corrections are taken into account for all measurements reported in this study.

Figure 4. Gamma Counting System.

Fast Neutron Flux Determination. The fast neutron flux is determined by activating and gamma counting a copper foil. For the purposes of this report "fast" neutrons will be taken to mean approximately 14.4-MeV neutrons.

Neutron activation of copper leads to the following reactions

$$^{63}Cu + n \rightarrow ^{62}Cu + 2n$$

$$T\frac{1}{2} = 9.9 \text{ minutes}$$

$$\rightarrow ^{62}Ni + \beta^+ (2.92 \text{ MeV})$$

The activated copper foil is sandwiched between 0.953-cm disks which annihilate the positrons causing the emission of two 0.511-MeV gammas per annihilation. These gammas are counted to measure the activity. The absorber thickness was chosen to conform to the "Texas Convention."[15]

Table 1 gives the essential physical and nuclear properties of the copper foil used in the analysis.

Table 1. Physical and Nuclear Properties of Copper Foil.

Thickness of foil	$x = 0.0254$ cm
Area of foil	$A = 5.0671$ cm^2
Density of copper	$\rho = 8.96$ g/cc
Isotopic abundance of ^{63}Cu	.6909
Average atomic weight of Cu	63.54 amu
Half life of ^{62}Cu decay	$T\frac{1}{2} = 9.9$ min.
β^+ emission per ^{62}Cu decay	.97
Cross section for (n,2n) reaction	$\sigma_p = 530$ mb$^{(a)}$
Number of ^{63}Cu nuclei per unit volume	$n_p = 5.8675 \times 10^{22}$ cm^{-3}
Decay constant for ^{62}Cu	$\lambda = 0.0011669$ sec^{-1}
Number of Cu nuclei per unit volume	$n_t = 8.4925 \times 10^{22}$ cm^{-3}
Total cross section	$\sigma_t = 2.88$ b$^{(a)}$

(a)Murrey D. Goldberg, et al., Neutron Cross Sections, BNL 325, 2nd Ed., Supp. No. 2, Vol. II-A, February, 1966.

The cross section is very energy dependent, and the energy of the neutrons depends on the angle at which they are emitted f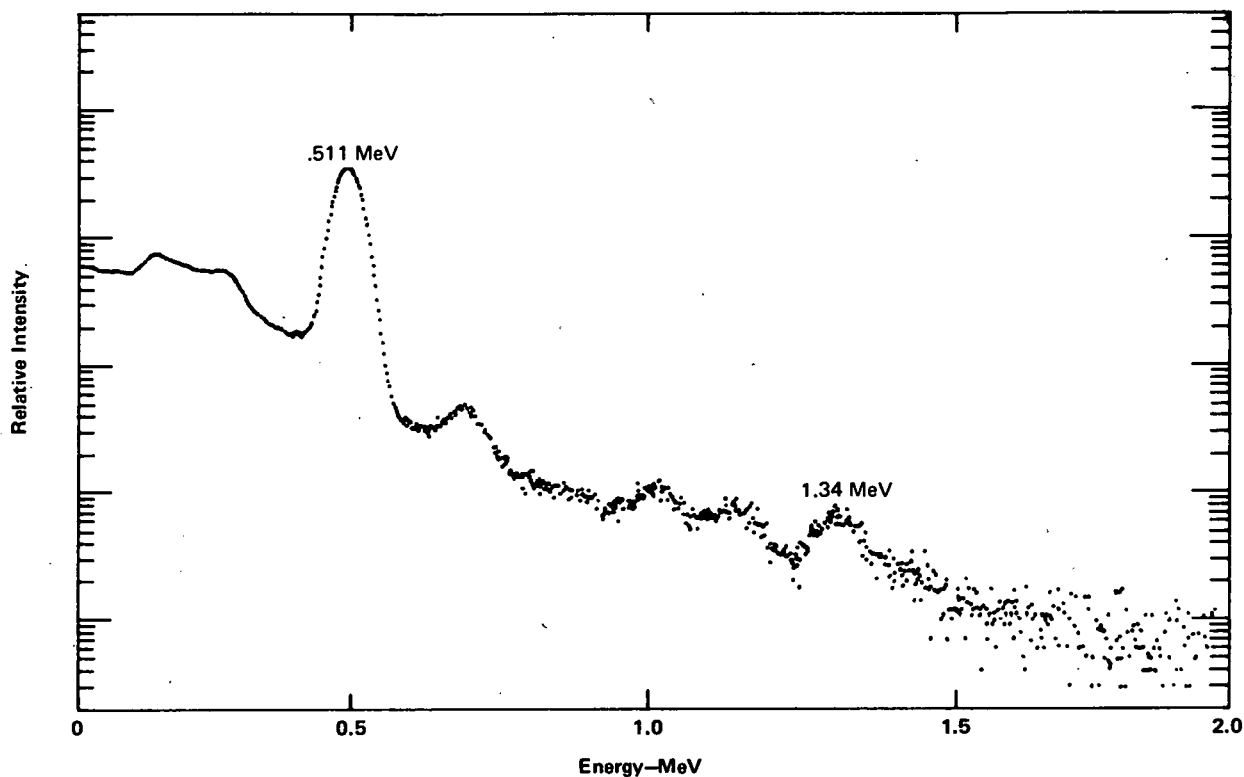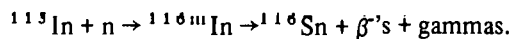rom the source. The value of 530 mb is for 14.4 MeV neutrons which are emitted at an angle of 45° from the accelerator beam.

The number of ^{63}Cu atoms per unit volume is calculated by the use of the formula

$$n_p = \frac{N_{AV} \cdot \rho \cdot (\text{isotopic abundance})}{(\text{atomic weight})},$$

where N_{AV} is Avogadro's number.

The counting factors for the fast neutron measurement are as follows:

1. Photopeak efficiency: For 0.511 MeV gammas detected by a 3-in.-diameter by 3-in.-thick NaI(Tl) crystal. $P = 0.625$[16]

2. Branching ratio: There are two 0.511 MeV gammas emitted per positron annihilation and 0.97 positrons emitted per decay of ^{62}Cu; thus, $\epsilon = 1.94$.

3. Absorption correction factor: For a lucite absorber and for 0.511 MeV gammas $\mu = 0.95$ cm^2/g. The density of lucite is 1.176 g/cm^3. The absorber completely surrounds the foil and thus the thickness used is the average thickness or $\Delta\xi = 0.9525$ cm. For copper $\mu = 0.084$ cm^2/g, $\rho = 8.96$ g/cm^3, and the average thickness $\Delta\xi = 0.0127$ cm. Using these parameters the absorption correction factor is a ≈ 0.8905.

4. Detector efficiency: The copper foils used are 2.54-cm diameter and are sandwiched between 0.953-cm-thick lucite absorbers. This whole assembly is the source of 0.511 MeV gammas. The source thickness thereby becomes 1.91 cm and the source to detector distance is 2.048 cm. The absorption coefficient $\tau = 0.32$/cm.[16] Using the computer program in Appendix II, the detector efficiency for the above arrangement was calculated to be q = 0.108.

The time intervals used for fast neutron measurements in this study are irradiation time $t_0 = 2$ minutes, transfer time $t_1 = 2$ minutes, and counting time $t_2 = 2$ minutes.

The error associated with the measurement of the fast neutron flux is estimated to be 5%.[18] An example of a copper gamma spectrum is given in Figure 5.

Figure 5. Gamma Spectrum of Copper-63.

Thermal Neutron Flux Determination. The thermal flux is determined by activating and counting an indium foil.

Neutron activation of the indium leads to the following reactions:

$$^{115}In + n \rightarrow {}^{116m}In \rightarrow {}^{116}Sn + \beta\text{'s} + \text{gammas}.$$

In the decay of ^{116}Sn to the ground state a number of gammas are emitted. One of the most prominent is a 1.29-MeV gamma. The area of the 1.29 MeV photopeak is used to determine the activity of the indium foil.

To stop the betas from entering the crystal and interfering with the counting results, a lucite absorber is placed between the indium foil and the detector.

The thickness required to stop the 1-MeV beta is approximately 0.38 cm.

Table 2 gives the essential properties of the indium used in this analysis.

Table 2. Physical and Nuclear Properties of Indium Foil.

Thickness of foil	$x = 0.0761$ cm
Area of foil	$A = 4.7875$ cm^2
Density of indium	$\rho = 7.31$ g/cc
Isotopic abundance of ^{115}In	.9572
Average atomic weight of In	114.82 amu
Half life of ^{116m}In decay	$T\frac{1}{2} = 54$ min.
Number of 1.29 gammas per ^{116m}In decay	.81
Cross section for (n,γ) reaction	$\sigma_p = 157$ b[a]
Number of ^{115}In nuclei per unit volume	$n_p = 3.67 \times 10^{22}$ cm^{-3}
Decay constant for ^{116m}In	$\lambda = 0.000213934$ sec^{-1}
Number of In nuclei per unit volume	$n_t = 3.83 \times 10^{22}$ cm^{-3}
Total cross section	$\sigma_t = 196$ b[a]

(a)Murrey D. Goldberg, et al., Neutron Cross Sections, BNL 325, 2nd Ed., Supp. No. 2, Vol. II-B, August, 1966.

The counting factors for the thermal neutron measurement are as follows:

1. Photopeak efficiency: For a 1.29-MeV gamma ray detected by a 3-in.-diameter by 3-in.-thick NaI(Tl) crystal, P = 0.355.[16]

2. Branching ratio: From the decay scheme of ^{116m}In[19] the average number of 1.29 MeV gamma rays produced per decay of the nucleus is 0.81. Therefore, ϵ = 0.81.

3. Absorption correction factor: For indium, μ = 0.052 cm^2/g, ρ = 7.31 g/cm^3, and $\Delta\xi$ = 0.381 cm. Therefore, a = 0.9587.

4. Detector efficiency: The indium foils used in this measurement are 2.54 cm in diameter and are placed 3.0 cm from the 3-in.-diameter by 3-in.-thick NaI(Tl) crystal. For a 1.29-MeV gamma ray the absorption coefficient is τ = 0.203 cm^{-1}.[16] Using the program given in Appendix II, the detector efficiency was calculated to be q = 0.08253.

The time intervals used in the thermal neutron flux determination are: irradiation time t_0 = 10 minutes, transfer time t_1 = 3 minutes, and counting time t_2 = 3 minutes.

The error associated with this measurement is approximately 3.5%.[18] An example of an indium gamma ray spectrum is given in Figure 6.

GRAPHITE MODERATOR

Thermal neutrons are used in most radiography work because neutrons in this energy range (0.01 - 0.30 eV) are relatively easy to detect and have desirable attenuation characteristics.

Figure 7 is an illustration of the moderating assembly of the neutron radiography system. The assembly is a

Figure 6. Gamma Spectrum of Indium-116^m.
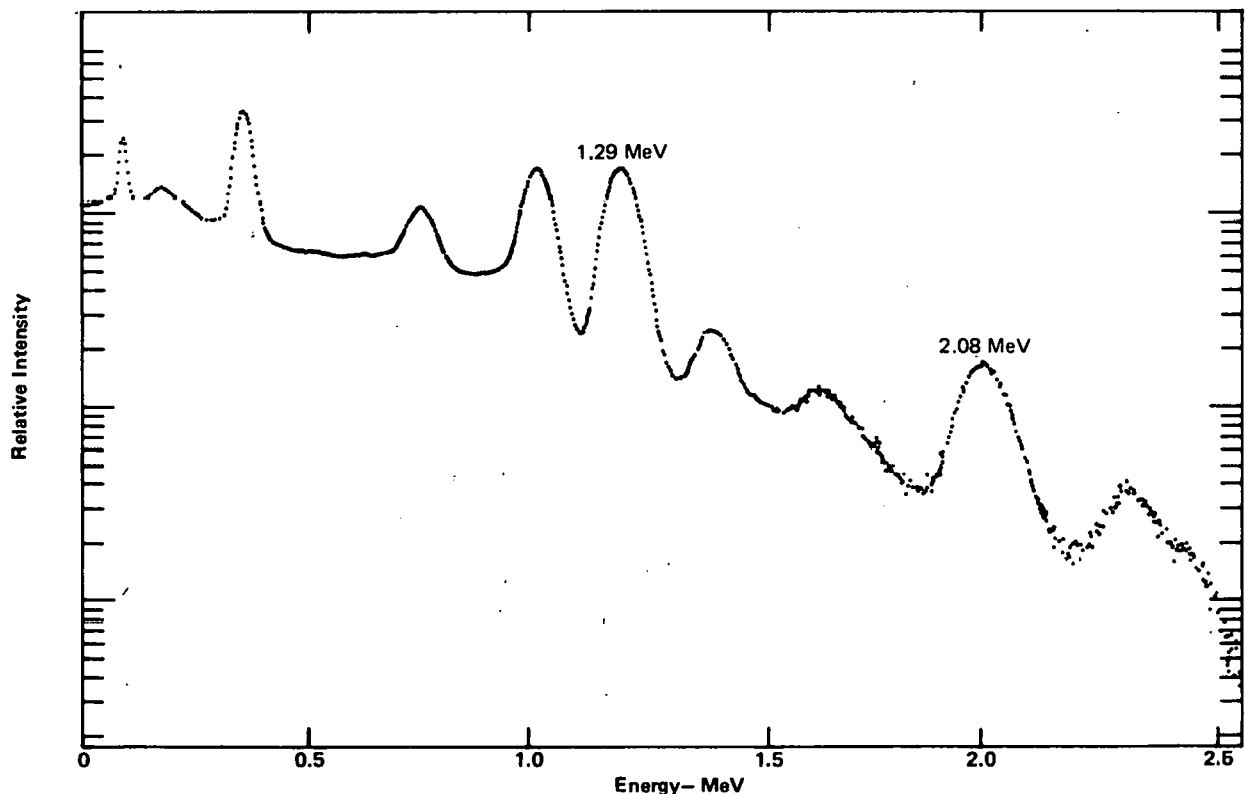
graphite right cylinder 76.2 cm in diameter and 76.2-cm high, in one end of which is located the sealed-tube fast neutron source.

1. CADMIUM LINED COLLIMATOR
2. ACCELERATOR HEAD POSITION
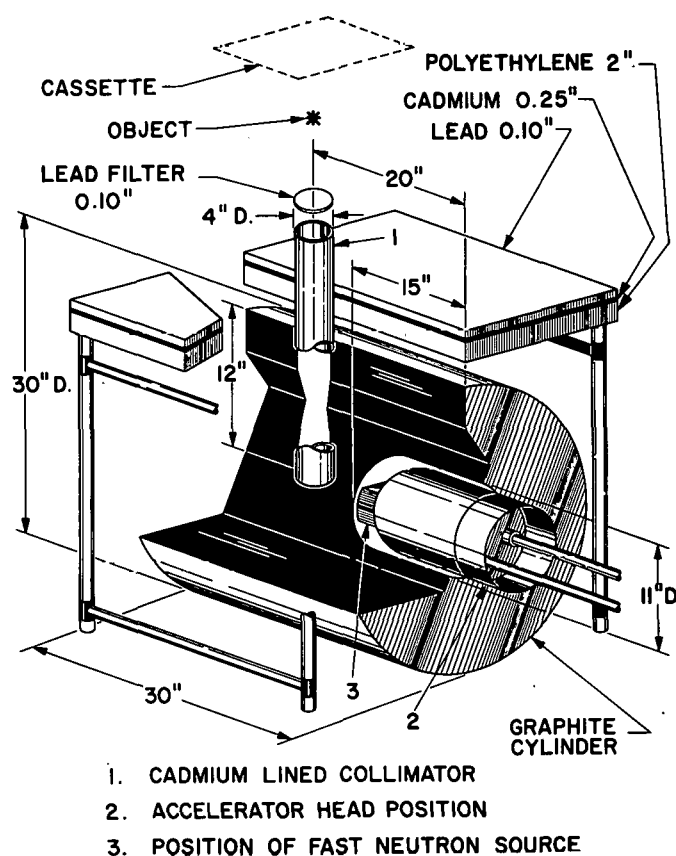3. POSITION OF FAST NEUTRON SOURCE

Figure 7. Graphite Moderator.

The radial neutron flux distribution for the bare system is presented in Figure 8.

The bare system includes only the fast neutron source and the graphite moderator. The radial points are measured normal to the axis of the graphite cylinder along the axis of the cadmium-lined collimator. The thermal neutron flux was calculated by subtracting the epithermal contributions from the total neutron flux measured by bare indium foils. The epithermal contri- bution was measured by surrounding an indium foil with 0.051 cm of cadmium to calculate a cadmium ratio which is approximately equal to the ratio of the total neutron intensity to the intensity of neutrons having an energy greater than 0.3 eV.
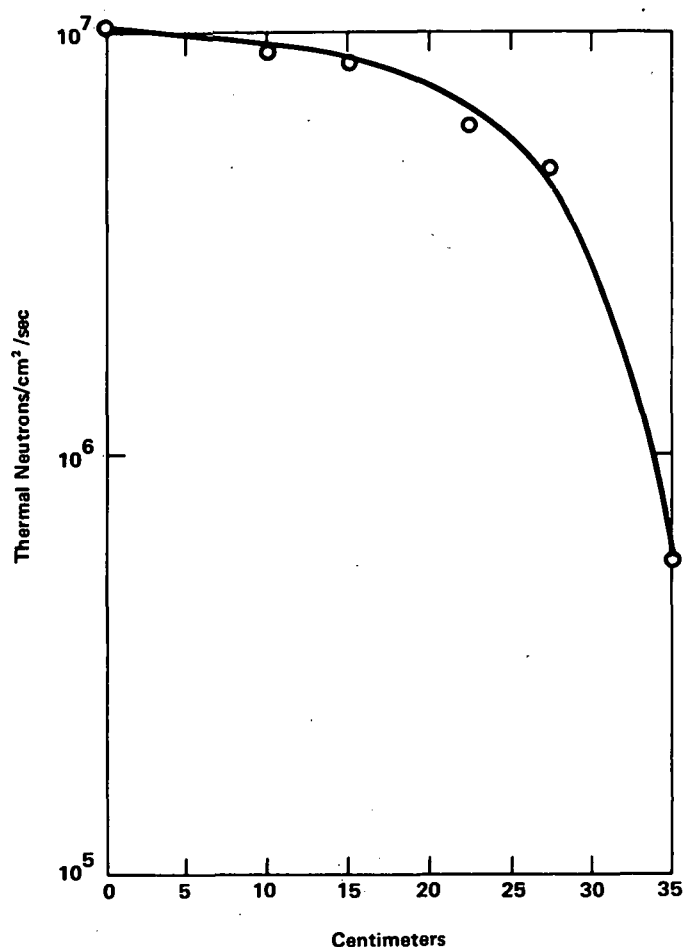

Figure 8. Radially-Outward Thermal Flux Distribution for Bare Graphite Moderator.

NEUTRON COLLIMATION AND THE SHIELD- ING OF X-RAYS

The characteristics of a neutron beam required for successful thermal neutron radiography should be considered. This beam must have the same character- istics required of the beam in X-ray radiography. The beam must be of sufficient intensity to yield an image that can be photographed. Also, the beam must be well collimated to provide the resolution required for a given inspection problem. Resolution, in this meaning, is the ability of the human eye to distinguish separate images of objects very close together.

A radiograph is defined to be "a shadow picture of an object that has been placed in the path of an X-ray or gamma-ray beam."[20] A collimated beam of thermal neutrons is extracted from the graphite moderator by a 4-in.-diameter void as shown in Figure 7. Added collimation is achieved with a cylindrical cadmium liner. The length of the liner is determined by the required

11

exposure time and film density. For all radiographs presented in this report, the collimator ratio (length: inlet aperture) was chosen to be 7.25.

Polyethylene, cadmium, and lead sheets are placed between the graphite and object position as shown in Figure 7. The thermal neutron leakage from the surface area of the moderator is on the order of 10^5 n/cm^2-sec, therefore the polyethylene and cadmium sheets are needed to prevent thermal neutrons not in the collimated beams from reaching the object to be radiographed. The polyethylene also serves to slow down to thermal energies some of the fast neutrons that escape the graphite moderator. Fast neutron effects on the radiographic film are therefore reduced.

During generator operation, X-rays are produced by the interaction of both fast and thermal neutrons with the sealed-tube, moderator material, polyethylene, and cadmium. It was experimentally determined that a 0.254-cm-thick lead sheet in conjunction with a 0.254-cm-lead filter, placed over the collimator opening, restricts the X-ray component of the beam to approximately 0.50 mr/sec at the object position. This was for a collimator ratio of 7.25. The X-ray intensity was determined by use of thermal luminescent dosimeter (TLD-600) crystals. The thermal neutron flux at the object position was 1.1×10^5 n/cm^2-sec. Thus, the ratio of the thermal neutron flux to the gamma radiation intensity was 2.2×10^5 n/cm^2-mr.

DETECTION OF THERMAL NEUTRONS

The method used in this report to detect thermal neutrons photographically makes use of ordinary X-ray film in conjunction with a converter screen. The converter screen absorbs thermal neutrons and promptly re-emits gamma radiation which is photographically more detectable than the neutron image. Neutrons, being uncharged particles, do not interact appreciably with the emulsion of X-ray film and it is necessary to activate a converter material to obtain an image.

Gadolinium is the converter material used for the radiographs presented in this report. The gadolinium is a 10.16- by 17.78- by 0.0025-cm sheet. Its interaction with thermal neutrons is represented by the two reactions: (1) ^{155}Gd(n,γ)^{156}Gd, and (2) ^{157}Gd(n,γ)^{158}Gd. The thermal neutron reaction cross section for (1) is 61,000b and for (2) is 254,000b.

The method which uses a converter screen like gadolinium is called the direct exposure method. Looking at
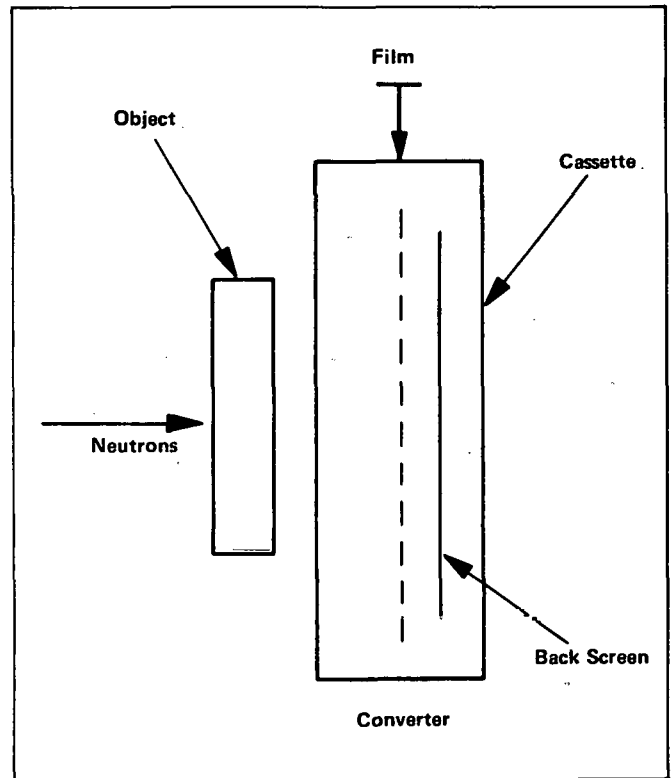

Figure 9. Direct Exposure Method.

Figure 9, we see that the film and the converter screen are placed together in the beam to detect the neutron image. This assembly is loaded into a vacuum cassette which serves to hold the film in intimate contact with the converter material (Figure 10). Aluminum is used as the cassette material to minimize thermal neutron activation gamma rays. The cassette is approximately 23 cm by 15 cm.

All neutron radiographs in this report were taken using the direct technique. The cassette was placed 73.66 cm from the base of the collimator void for a collimator ratio of 7.25. The cadmium ratio at the object position was determined to be 3.5.

CHARACTERISTIC CURVES FOR KODAK TYPE AA AND TYPE NS FILMS

Characteristic curves for Kodak Type AA and Type NS films are presented in Figure 11. These films are the most commonly used films for low-flux thermal neutron radiography. The response of these films to X-rays is described in detail in reference 20.
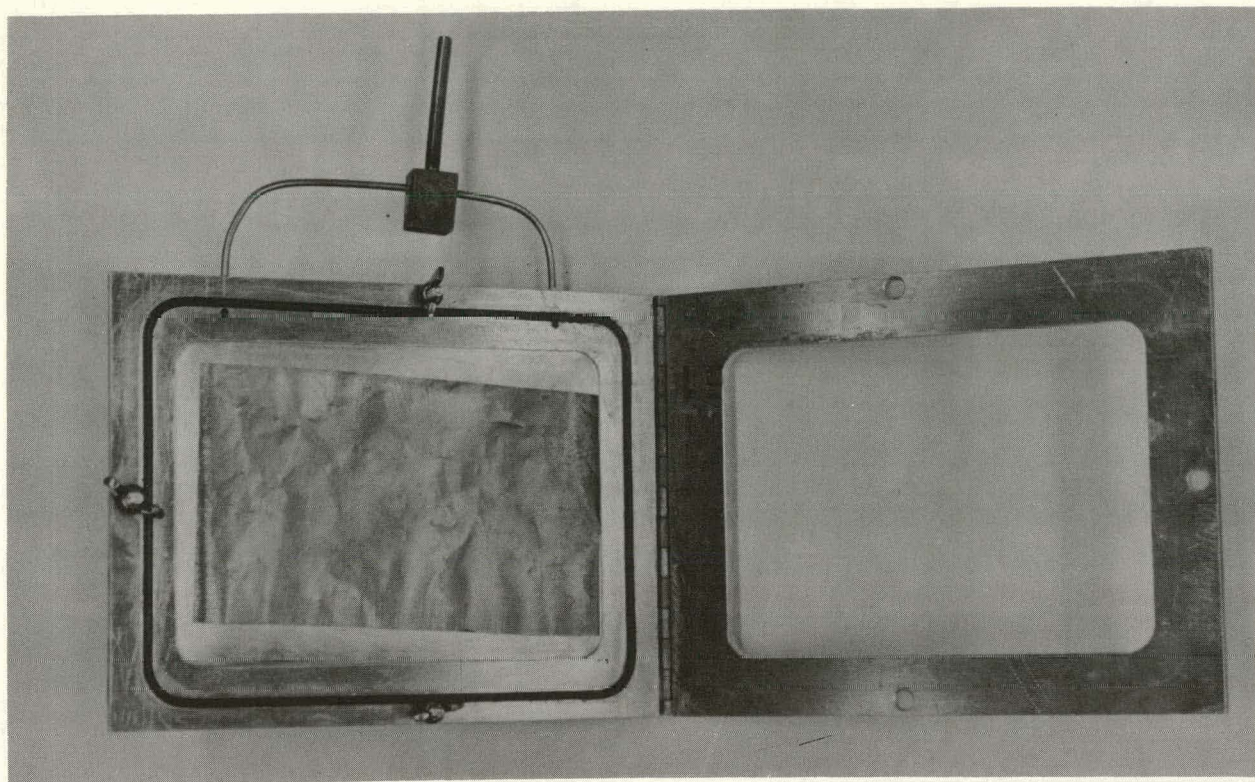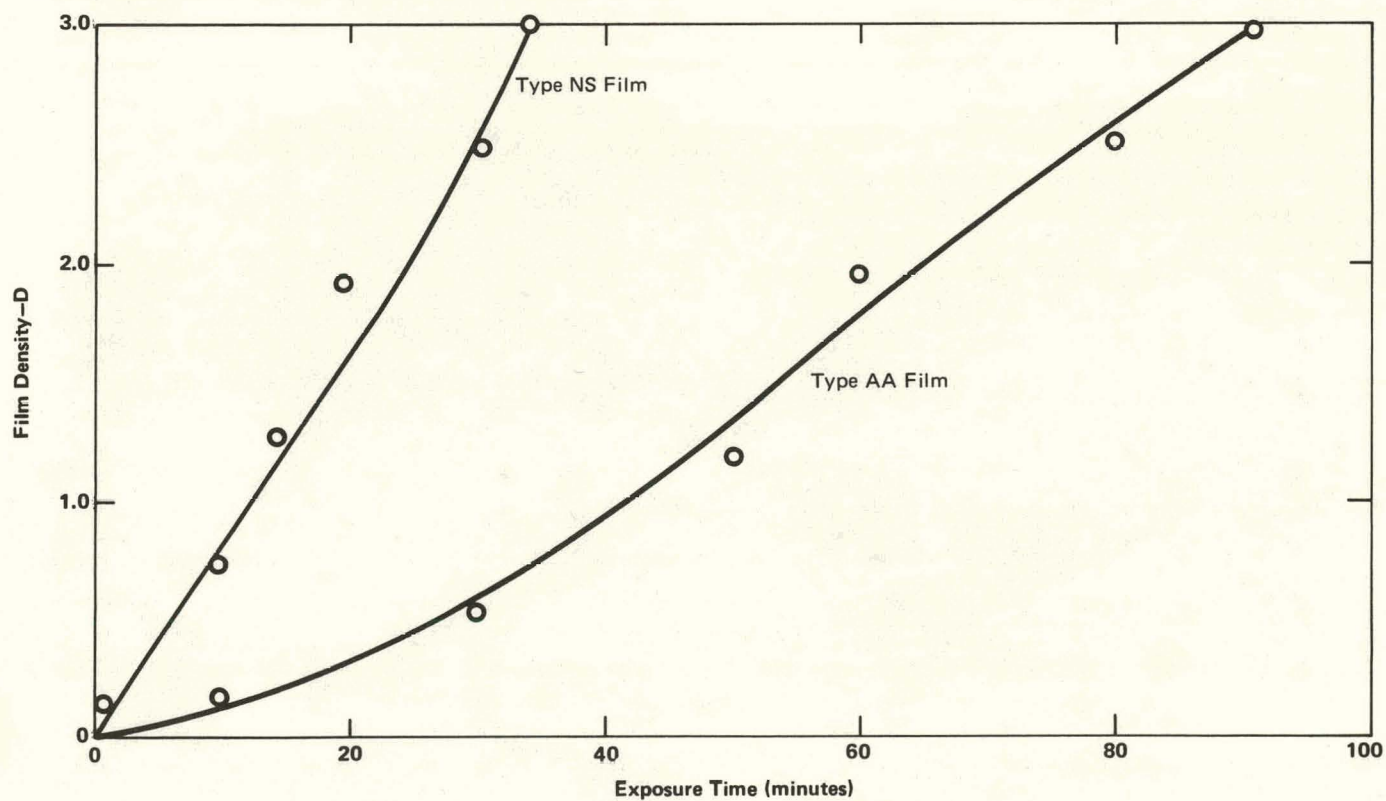
Figure 10. Aluminum Vacuum Cassette Showing 0.0025 cm Gadolinium Back Screen.

Figure 11. Characteristic Curves for Kodak Type AA and Type NS Films.

A characteristic curve "expresses the relationship between the exposure applied to a photographic material and the resulting photographic density."[12] Density is defined by the equation

$$D = \log_{10} \frac{I_o}{I_t},$$

where D is the density, I_o is the incident intensity, and I_t is the transmitted intensity of the light beam in the densitometer used to measure the film density.

EXAMPLES OF THERMAL NEUTRON RADIOGRAPHS

Figure 12 is a photograph of all the specimens included in the radiographs of this report. These include a 0.95-cm-thick cigarette lighter, a 1.3-cm-thick stainless steel gas outlet fixture in which a neoprene O-ring was inserted, a rubber O-ring, a lead number "2", a cadmium image quality indicator (IQI), and three

cartridges (.45, .30-30, and .308 caliber). The holes in the IQI are 0.10 cm in diameter and are spaced 0.0025, 0.0051, 0.0076, 0.013, 0.025, 0.051, and 0.076 cm apart. The IQI is 0.159 cm thick.

Figure 13 is a neutron radiograph of the cigarette lighter, IQI, lead number "2", rubber O-ring, and the gas outlet fixture. Type AA film was used with an exposure time of 90 minutes at a thermal beam flux of 1.1×10^5 n/cm²-sec. The film density produced by the X-ray component in the beam was measured to be 0.10. All neutron radiographs in this report were developed in an automatic film processor. In a separate neutron radiograph, the IQI was placed 0.064 cm from Kodak Type AA film for an exposure of 90 minutes at a thermal beam flux of 1.1×10^5 n/cm²-sec. The resolution was determined to be 0.025 cm.

An X-ray of the specimens of Figure 12 is shown in Figure 14. This radiograph was taken with a 300 keV X-ray generator at 145 keV. The film load was 5RR5 with an exposure of 15 mas. The resolution of this X-ray is 0.0025 cm.

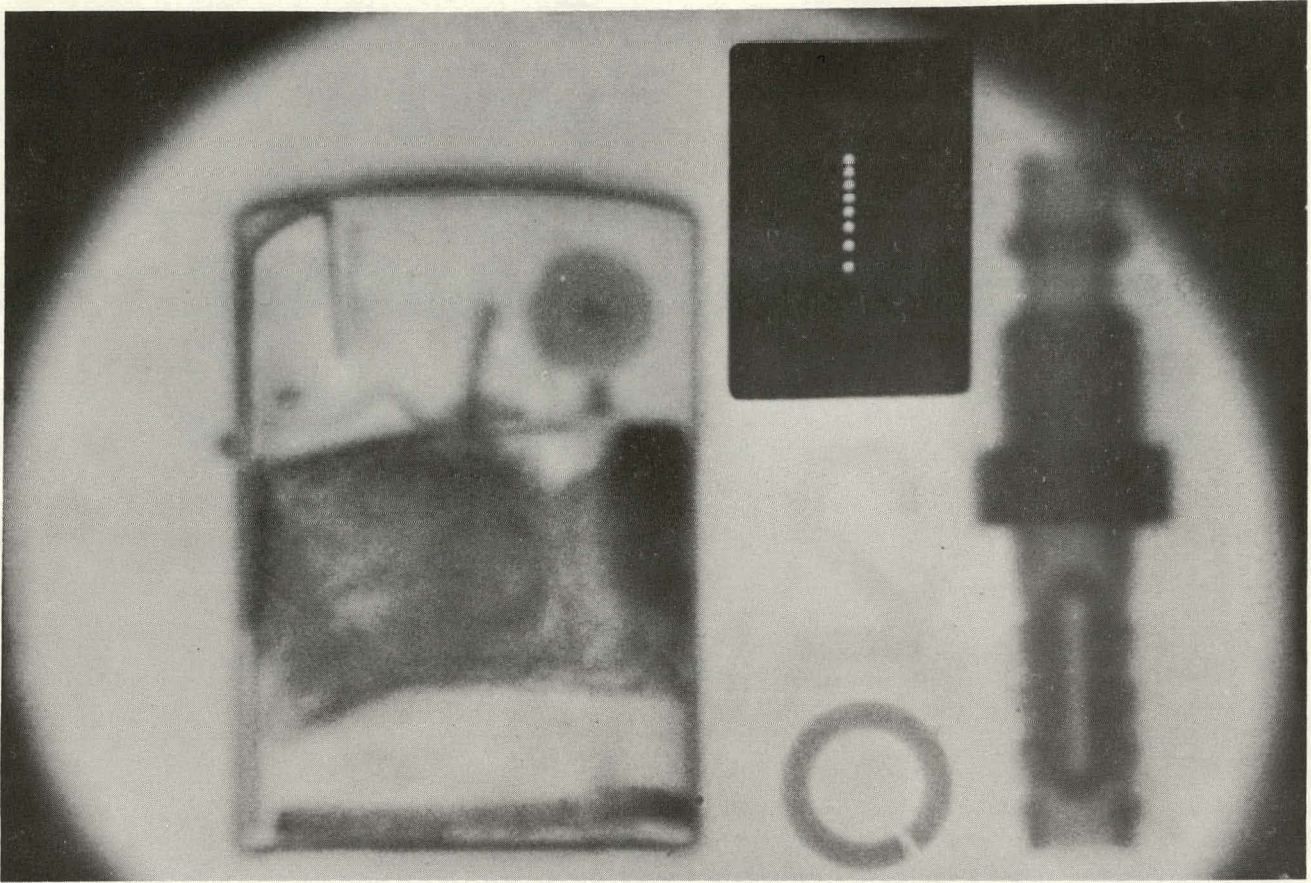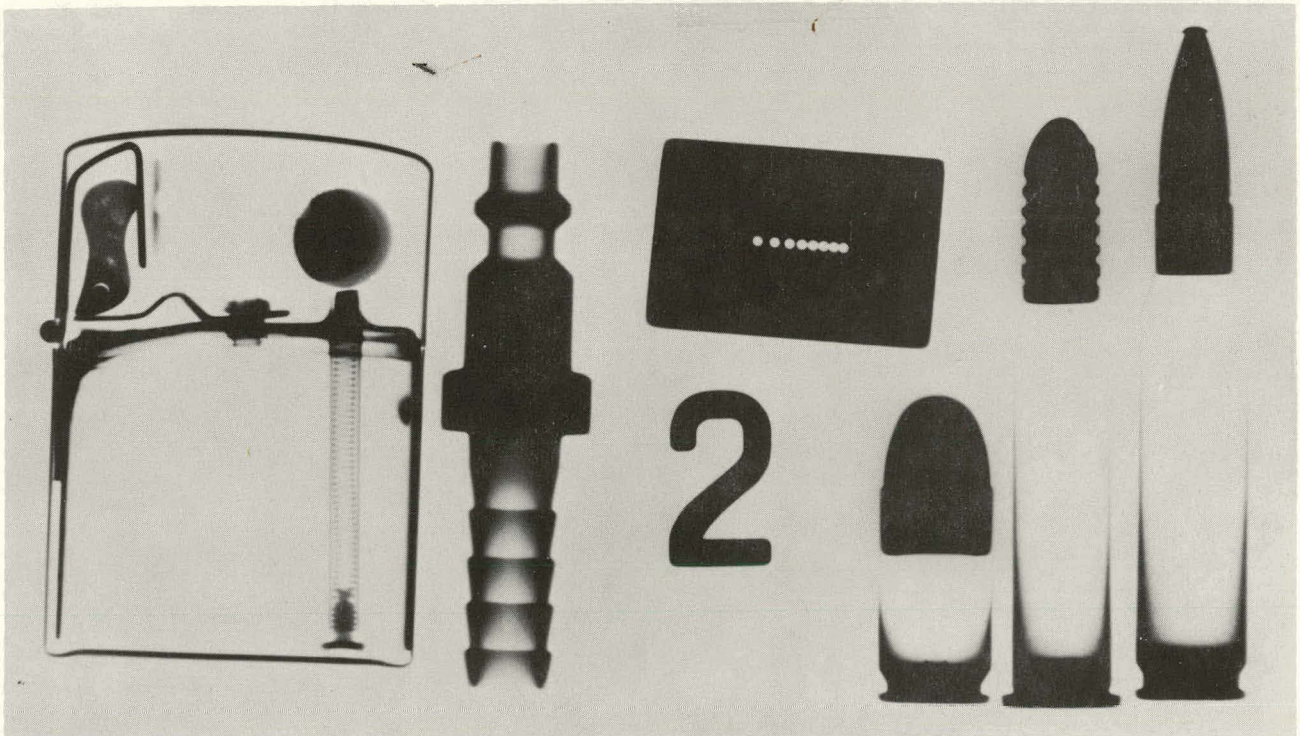Figure 12. Photograph of Specimens Presented in the Neutron Radiographs.
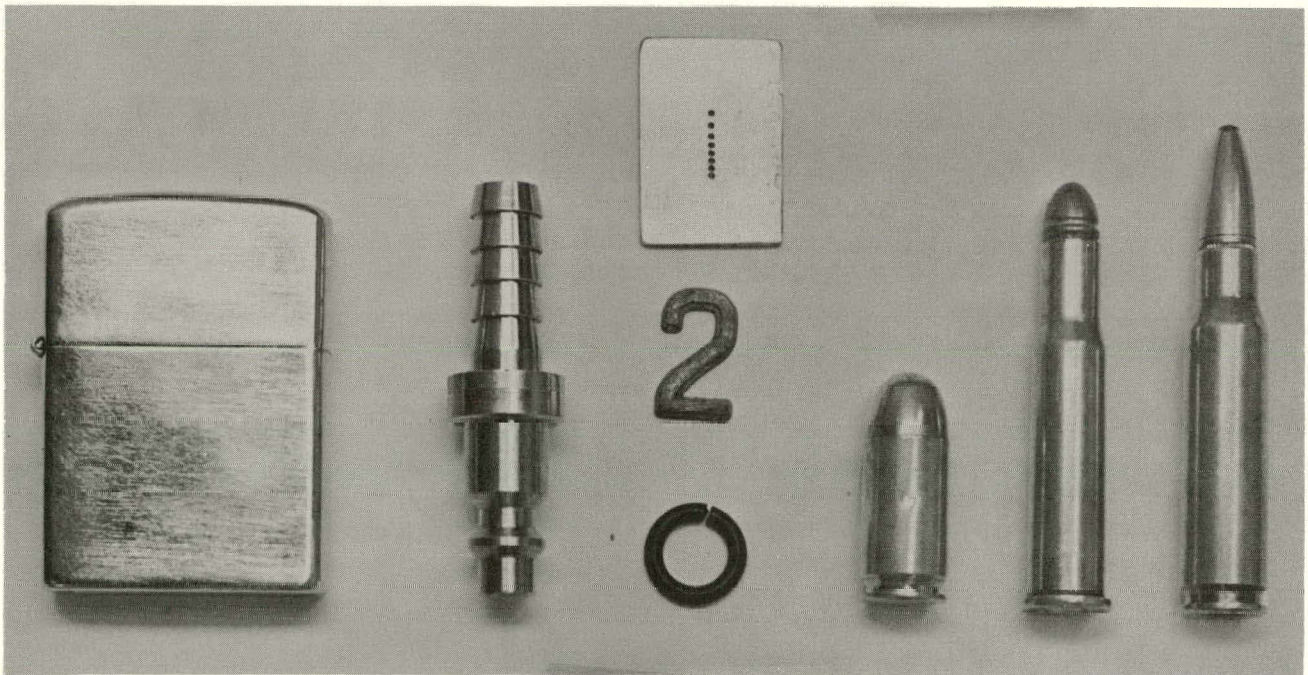
Figure 13. Neutron Radiograph using 0.0025-cm Gd Converter Screen with Kodak Type AA Film.

Figure 14. X-ray of Objects in Figures 13 and 15.

In Figure 13, the neoprene O-ring in the gas outlet fixture is clearly visible as compared to the X-ray of the same object in Figure 14. Also, the X-ray radiograph of the cigarrette lighter fails to show the cotton or wick. The cotton and wick contain hydrogen which readily attenuates thermal neutrons. The lead number "2" is hardly visible in the neutron radiograph while in the X-ray radiograph it is outstanding. This shows the penetrating ability of the neutron beam in heavy elements and also demonstrates how neutron and X-ray radiography complement each other. The rubber O-ring (which also contains large amounts of hydrogen) is not visible in the X-ray radiograph while in the neutron radiograph it is very outstanding.

Figure 15 is a neutron radiograph of a .45 caliber cartridge, a hand-loaded .30-30 caliber cartridge, and a .308 caliber soft-point cartridge. The .308 caliber has a standard 150-grain load with a copper jacket on the lead bullet.

The .30-30 caliber is purposely light-loaded without any jacket on the lead bullet. The .45 caliber is a no-load shell with a copper jacket around the lead bullet. The IQI, rubber O-ring, and lead number "2" are also included in this thermal neutron radiograph. The resolution was determined to be 0.025 cm. Type AA film was used with an exposure of 90 minutes at a thermal beam flux of 1.1×10^5 n/cm^2-sec. An X-ray radiograph of these specimens is shown in Figure 14.

Of particular interest is the comparison of the .30-30 caliber cartridge in the neutron radiograph and the X-ray radiograph. In the neutron radiograph of the .30-30 caliber, the grease in the grease rings is clearly visible. However, in the X-ray radiograph, only the rings are visible. The neutron radiograph also reveals the differences of the powder densities between the three cartridges. Notice in the .308 caliber cartridge that the powder has collected along one edge of the shell. This is caused by the cassette being loaded in a horizontal position.

Figure 15. Neutron Radiograph using 0.0025 cm Gd Converter Screen with Kodak Type AA Film.
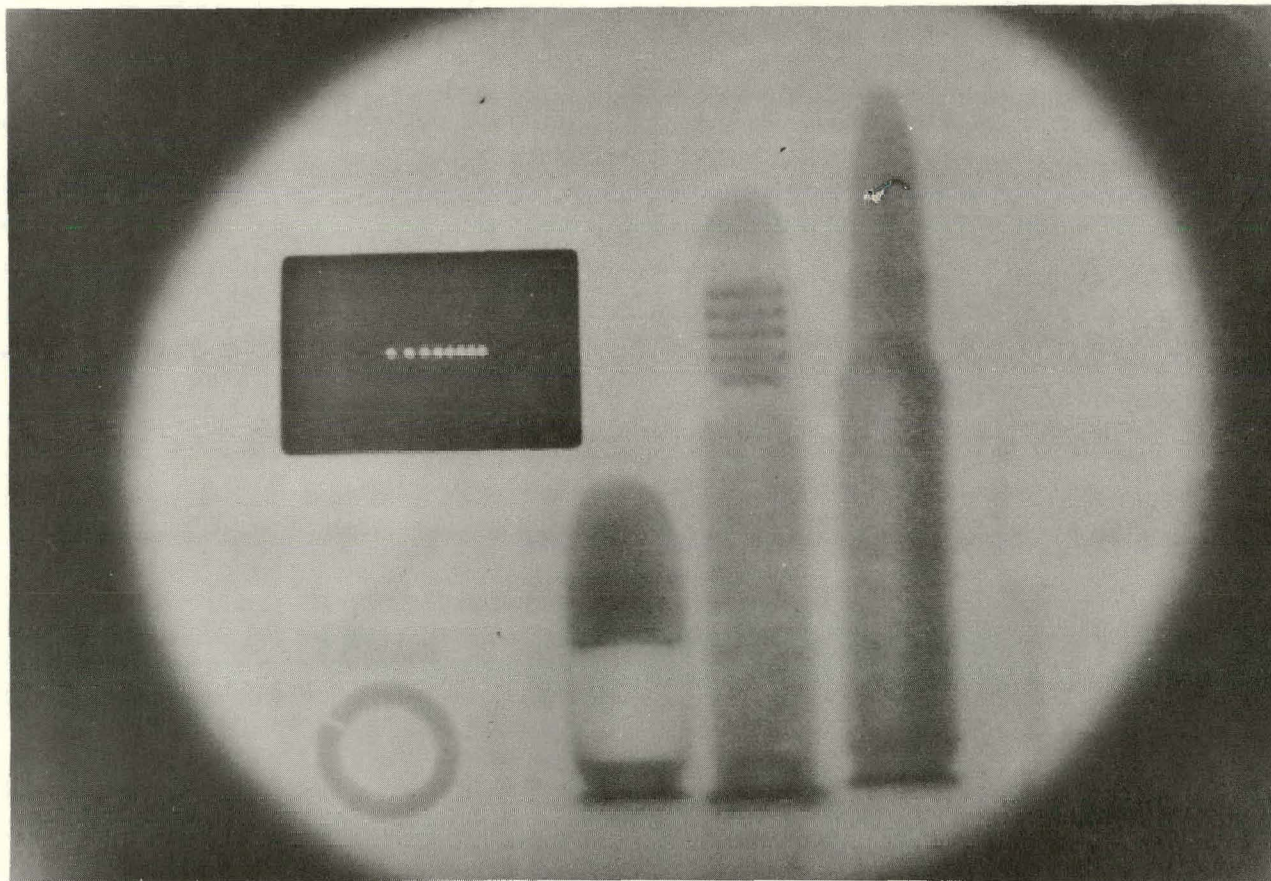
REFERENCES

1. H. Kallman, Neutron Radiography: Res., *V 1*, p 254-260, 1947.

2. J. Thewlis, "Neutron Radiography," *Brit. J. Appl. Phys.*, *V 7*, p 345-350, 1956.

3. J. Thewlis, "Neutron Radiography: Progress in Non-Destructive Testing," Heywood, Ltd., London, *V 1*, p 111-126, 1958.

4. O. Peter, "Neutronen-Durchlenchtung;" *Zeitschr. Naturforsch, V 1*, p 557-559, 1946.

5. J. Thewlis and R. T. P. Derbyshire, Report AERE M/TN 37, U. K. Atomic Energy Establishment, Harwell, England, 1956.

6. H. Berger and W. N. Beck, "Neutron Radiographic Inspection of Radioactive Irradiated Reactor Fuel Specimens," *Nucl. Sci. Eng., V 15*, p 411, 1963.

7. G. Olive, J. F. Cameron, and C. G. Clayton, A Review of High Intensity Sources and their Application in Industry, AERE-R3920, U. K. Atomic Energy Research Establishment, Wantage Research Laboratory, England, 1962.

8. H. Berger, "Neutron Radiography-Methods, Capabilities, and Applications," Elsevier Publishing Company, New York, N. Y., 146 p, 1965.

9. C. B. Shaw and J. L. Cason, "Portable Neutron Radiographic Camera using ^{252}Cf," BNWL-SA-3090, 17 p, 1970.

10. F. A. Iddings, "Low-Voltage-Accelerator Neutron Radiography," *Isotop. Radiat. Technol., V 7*, No. 3, p 291, 1970.

11. J. P. Barton, "Neutron Radiography using Nonreactor Sources," *Isotop. Radiat. Technol., V 6*, No. 2, p 149-153, 1969.

12. D. E. Wood, "The Application of Fast-Neutron Generators to Neutron Radiography," Kaman Nuclear Technical Note No. 115, 1967.

13. G. Breynat and M. Dubus, "Utilization of Small Accelerator Neutron Generators in Neutron Radiography," *Mater. Eval., V 27*, No. 10, p 220, 1969.

14. J. P. Barton, "Divergent Beam Collimator for Neutron Radiography," *Mater. Eval., V 25*, p 45A, 1967.

15. The Texas Convention on the Measurement of 14 MeV Neutron Fluxes from Accelerators with Appendix by R. L. Heath, Proceedings of the 1965 International Conference on Modern Trends in Activation Analysis, College Station, Texas, 1965.

16. R. L. Heath, Scintillation Spectrometer, Gamma-Ray Spectrum Catalogue, AEC Research and Development Report IDO-16880-1, Appendix III, 1964.

17. H. A. Enge, "Introduction to Nuclear Physics," Addison-Wesley Publishing Company, Inc., Reading, Massachusetts, 1966.

18. R. L. Murri and D. G. Vasilik, "Error Analysis of Neutron Flux Measurements Determined by Foil Activation Analysis," Rocky Flats Division, The Dow Chemical Company, Golden, Colorado, (to be published), 1971.

19. C. M. Lederer, J. M. Hollander, and I. Perlman, Table of Isotopes, 6th ed., John Wiley and Sons, Inc., New York, N. Y., 1968.

20. Eastman Kodak Company, "Radiography in Modern Industry," Eastman Kodak Company, Rochester, N. Y., 2nd ed., 136 p, 1957.

APPENDIX I. DERIVATION OF DETECTOR EFFICIENCY

The detector efficiency is a combination of the geometry factor and the absorption factor. In this derivation, the geometry factor will be derived first and then combined in the proper way with the absorption factor. The various quantities used in the derivation are shown in Figure I-1.
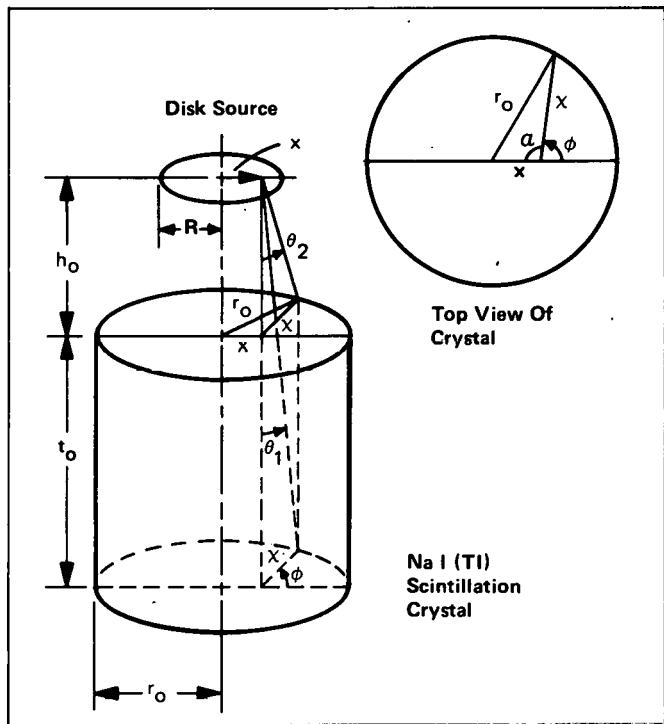

Figure I-1. Source and Detector Geometry.

The geometry factor is the solid angle subtended by the detector at the source, divided by 4π. For a point source the geometry factor G is given by

$$G = \frac{1}{4\pi}\int_0^{2\pi}\int_0^{\theta} \sin\theta\, d\theta\, d\phi.$$

For a disk source of Radius R,

$$G = \frac{1}{4\pi\cdot\pi R^2}\underbrace{\int_0^R\int_0^{2\pi} x\,dx\,da}_{\substack{\text{Integral}\\\text{over disk area}}} \underbrace{\int_0^{2\pi}\int_0^{\theta}\sin\theta\, d\theta\, d\phi.}_{\substack{\text{Solid Angle}\\\text{Integral}}}$$

The integral over a can be done immediately, and by symmetry, ϕ may be integrated from o to π and multiplied by 2. Thus the above expression can be written as

$$G = \frac{1}{\pi R^2}\int_0^R x\,dx \int_0^{\pi} d\phi \int_0^{\theta}\sin\theta\, d\theta.$$

This expression must be combined with the absorption factor, which is the ratio of photons absorbed in the crystal to the number of photons impinging on the crystal. Let I_0 be the number of photons impinging on the crystal. Then the number passing through the crystal is given by

$$I = I_0\, e^{-\tau\psi}.$$

where τ is the absorption coefficient and ψ is the thickness of the crystal traversed by the photons. The number absorbed is thus

$$I_0 - I = I_0(1-e^{-\tau\psi}),$$

and the absorption factor is the ratio

$$\frac{I_0(1-e^{-\tau\psi})}{I_0} = (1-e^{-\tau\psi}).$$

The detector efficiency is then given by

$$q = \frac{1}{\pi R^2}\int_0^R x\,dx \int_0^{\pi} d\phi \int_0^{\theta} (1-e^{-\tau\psi})\sin\theta\, d\theta.$$

The photon path length in the crystal ψ must be further defined in terms of the angles θ and ϕ. Consider the top view of the crystal as shown in Figure I-1. Using the Law of Cosines,

$$r_0^2 = x^2 + \chi^2 - 2x\chi \cos a$$

but

$$\phi + a = \pi$$

and

$$\cos a = \cos(\pi-\phi) = -\cos \phi.$$

Thus

$$r_o^2 = x^2 + \chi^2 - 2x\chi \cos \phi.$$

Rearranging terms and solving for χ by the quadratic formula gives

$$\chi = - x \cos \phi + \sqrt{x^2 \cos^2 \phi + r_o^2 - x^2}.$$

Again referring to Figure I-1, angles θ_1 and θ_2 are given by

$$\theta_1 = \tan^{-1}\frac{\chi}{t_o+h_o} \text{ and } \theta_2 = \tan^{-1}\frac{\chi}{h_o}.$$

By simple geometry then

$$\psi = \frac{t_o}{\cos \theta} \text{ for } 0 \leq \theta \leq \theta_1,$$

and

$$\psi = \frac{\chi}{\sin \theta} - \frac{h_o}{\cos \theta} \text{ for } \theta_1 \leq \theta \leq \theta_2.$$

Substituting these values for ψ into the expression for the detector efficiency gives

$$q = \frac{1}{\pi R^2} \int_0^R x dx \int_0^\pi d\phi \left\{ \int_0^{\theta_1} (1-e^{-\tau \cdot t_o \cos \theta}) \sin \theta d \theta \right.$$

$$\left. + \int_{\theta_1}^{\theta_2} \left(1-e^{-\tau(\chi\sin \theta - h_o/\cos \theta)}\right) \sin \theta d \theta \right\}.$$

Vegors et al.* uses a slightly different form of the above equation. The principle axis for the angle ϕ is shown in Figure I-2. By the Law of Cosines

$$r_o^2 = x^2 + \chi^2 - 2x\chi \cos a .$$
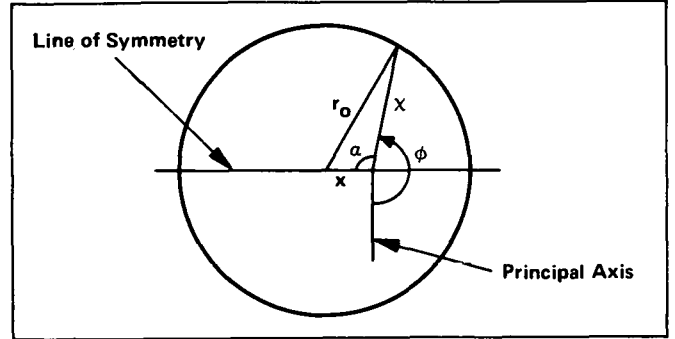
But

$$\phi + a = \frac{3\pi}{2}$$

*S. H. Vegors et al., Calculated Efficiencies of Cylindrical Radiation Detectors, AEC Report IDO-16370 (1958).

Figure I-2. Top View of Crystal Showing Heath's Modification.

so

$$\cos a = \cos \pi-(\phi-\pi/2) = -\cos(\phi-\pi/2)$$

$$= -\cos(\pi/2-\phi) = -\sin \phi.$$

Thus

$$r_o^2 = x^2 + \chi^2 + 2x\chi \sin \phi.$$

Solving for χ gives

$$\chi = -x \sin \phi + \sqrt{x^2 \sin^2 \phi + r_o^2 - x^2}$$

Now in order to preserve symmetry the integral over ϕ must go from $-\pi/2$ to $\pi/2$ or from $\pi/2$ to π.

If the source is thick then the expression for the geometry factor is extended to include the thickness and is given by

$$G = \frac{1}{4_n \cdot_n R^2 \cdot t} \underbrace{\int_0^T \int_0^R \int_0^{2\pi} \chi dx dy da}_{\text{Integral over disk volume}} \underbrace{\int_0^{2\pi} \int_0^\theta \sin \theta d \theta d\phi}_{\text{Solid Angle integral}}.$$

The development of this expression is identical to that given above. Therefore, the final expression for a source of thickness t is

$$q = \frac{1}{\pi R^2 t} \int_0^T dy \int_0^R x dx \int_0^\pi d\phi \left\{ \int_0^\theta (1-e^{-\tau t_o/\cos \theta}) \sin \theta d \theta \right.$$

$$\left. + \int_{\theta_1}^{\theta_2} \left(1-e^{-\tau(\chi/\sin \theta-h/\cos \theta)}\right) \sin \theta d \theta \right\} ,$$

where $h = h_o + y$ and all other variables are defined as before.

APPENDIX II. A PROGRAM TO CALCULATE THE DETECTOR EFFICIENCY
OF A SODIUM IODIDE CRYSTAL

```
1 C    EFFIC--A PROGRAM TO CALCULATE THE DETECTOR EFFICIENCY OF A
2 C    SODIUM IODIDE CRYSTAL.  RO IS THE RADIUS OF THE DETECTOR, R
3 C    IS THE RADIUS OF THE DISK SOURCE, HO IS THE DISTANCE FROM
4 C    THE SOURCE TO THE DETECTOR, TO IS THE THICKNESS OF THE
5 C    DETECTOR, AND TAU IS THE ABSORPTION COEFFICIENT OF THE NAI(TL)
6 C    CRYSTAL AND IS ENERGY DEPENDENT.  T IS THE SOURCE THICKNESS.
7 C
8 C
9 C
1 0C   NUMERICAL INTEGRATION OF NAI(TL) DETECTOR EFFICIENCY
1 1C
100    DIMENSION CONST(19)
110    PRINT 40,
120    PRINT 50,
130    PRINT ,
140    CALL OPENF(1, "EFFICD")
150    READ(1,) N
160    DO 100 IP=1,N
170    READ(1,) RO, TO, R, T, HO, TAU
180    M = 19
190    IF(T.EQ.0.0) M = 1
200    CONST(1) = 1.0
210    CONST(2) = 5.0
220    CONST(3) = 1.0
230    CONST(4) = 6.0
240    CONST(5) = 1.0
250    CONST(6) = 5.0
260    CONST(7) = 2.0
270    CONST(8) = 5.0
280    CONST(9) = 1.0
290    CONST(10) = 6.0
300    CONST(11) = 1.0
310    CONST(12) = 5.0
320    CONST(13) = 2.0
330    CONST(14) = 5.0
340    CONST(15) = 1.0
350    CONST(16) = 6.0
360    CONST(17) = 1.0
370    CONST(18) = 5.0
380    CONST(19) = 1.0
390    PI = 3.1415926536
400    TOTINT = 0.0
410    DO 35 L=1,M
420    AL = L
430    Y = (AL - 1.0) * (T / 18.0)
440    H = HO + Y
450    RINT = 0.0
460    DO 30 I=1,19
470    AI = I
480    X = (AI - 1.0) * (R / 18.0)
490    PHIINT = 0.0
500    DO 20 J=1,19
```

```
     N   = THE NUMBER OF DATA SETS
     RO  = RADIUS OF THE DETECTOR
     TO  = THICKNESS OF DETECTOR
      R  = RADIUS OF SOURCE
      T  = THICKNESS OF SOURCE
     HO  = DISTANCE FROM SOURCE TO DETECTOR
    TAU  = ABSORPTION COEFFICIENT OF
           NAI(TL) CRYSTAL
         = 0.32 FOR 0.511 MEV GAMMAS
         = 0.203 FOR 1.29 MEV GAMMAS

 ALL VALUES OF THE INPUT DATA MUST BE
 IN CENTIMETERS.  THE OUTPUT DATA IS
 ALSO IN CENTIMETERS.  THE INPUT DATA
 IS STORED UNDER THE FILE NAME "EFFICD".
```

```
510 AJ = J
520 PHI = -PI/2.0 + (AJ - 1.0) * (PI / 18.0)
530 XCAP = -X*SIN(PHI) + SQRT(X+2*(SIN(PHI))+2 + RO+2 - X+2)
540 ARG1 = XCAP / (H + TO)
550 ARG2 = XCAP / H
560 THETA1 = ATAN(ARG1)
570 THETA2 = ATAN(ARG2)
580 XINT1 = 0.0
590 XINT2 = 0.0
600 DO 10 K=1,19
610 AK = K
620 THETAO = (AK - 1.0) * (THETA1 / 18.0)
630 THETA = THETA1 + (AK - 1.0) * (THETA2 - THETA1) / 18.0
640 XINT1 = XINT1 + CONST(K) * SIN(THETAO) * (1.0 - EXP(-TAU *
650& TO /  COS(THETAO)))
660 10 XINT2 = XINT2 + CONST(K) * SIN(THETA) * (1.0 - EXP(-TAU *
670& (XCAP/SIN(THETA) - H/COS(THETA))))
680 20 PHIINT = PHIINT + CONST(J) * ((THETA1/60.0) * XINT1 +
690& ((THETA2 - THETA1)/60.0) * XINT2)
700 30 RINT = RINT + CONST(I) * (X * (PI/60.0) * PHIINT)
710 35 TOTINT = TOTINT + CONST(L) * ((R/60.0) * RINT)
720 G = ((T/60.0) * TOTINT) / (PI * R * R * T)
730 IF(T.EQ.0.0) G = TOTINT / (PI * R * R)
740 RO = RO * 2.0
750 R = R * 2.0
760 PRINT 60, RO, TO, R, T, HO, TAU, G
770 40 FORMAT(4X, "DETECTOR", 8X, "SOURCE", 33X, "DETECTOR")
780 50 FORMAT(3X, "DIA    TO", 7X, "DIA     T", 10X, "HO", 9X, "TAU",
790& 7X, "EFFICIENCY")
800 60 FORMAT(1X, F5.2, 2X, F5.2, 4X, F5.2, 2X, F5.2, 6X, F5.2, 6X,
810& F6.3, 5X, E12.6)
820 100 CONTINUE
830 PRINT, +2
840 END
```

INPUT

```
100 2
110 3.81, 7.62, 1.27, 1.905, 2.0475, 0.32
120 3.81, 7.62, 1.27, 0.0, 3.0, 0.203
```

OUTPUT

DETECTOR		SOURCE				DETECTOR
DIA	TO	DIA	T	HO	TAU	EFFICIENCY
7.62	7.62	2.54	1.91	2.05	0.320	0.107499E+00
7.62	7.62	2.54	0.00	3.00	0.203	0.825311E-01